doi:10.2533/chimia.2012.791 Chimia 66 (2012) 791–797 © Schweizerische Chemische Gesellschaft

NMR Spectroscopy in Bioinorganic Chemistry

Daniela Donghi, Silke Johannsen, Roland K. O. Sigel*, and Eva Freisinger*

Abstract: Multinuclear and multidimensional nuclear magnetic resonance (NMR) spectroscopy is applied in our groups to gain insights into the role of metal ions for the function and structure of large biomolecules. Specifically, NMR is used i) to investigate how metal ions bind to nucleic acids and thereby control the folding and structure of RNAs, ii) to characterize how metal ions are able to stabilize modified nucleic acids to be used as potential nanowires, and iii) to characterize the formation, structure, and role of the diverse metal clusters within plant metallothioneins. In this review we summarize the various NMR experiments applied and the information obtained, demonstrating the important and fascinating part NMR spectroscopy plays in the field of bioinorganic chemistry.

Keywords: Bioinorganic chemistry · NMR spectroscopy

1. Introduction

The research in our groups focuses on the elucidation of the delicate and manifold interactions of metal ions with different classes of nucleic acids and proteins as well as their role in folding, structure, and mechanism. On the one hand, we aim to understand the way in which metal ions and their complexes interact with large RNAs and (modified) DNAs. On the other hand, we investigate plant metallothioneins (MTs), in particular the formation and large structural variety of their metal cluster structures as well as their potential physiological functions.

Aside from NMR, we use multiple spectroscopic techniques such as UV-Vis, CD, fluorescence, and single molecule Förster Resonance Energy Transfer (smFRET).[1–5] In addition, classical biochemical assays like in-line probing analyses or Tb^{3+} cleavage assays are applied for the study of RNA, while application of mass spectrometry, MCD, and EXAFS forms an integral part of our research on plant MTs. Nuclear magnetic resonance (NMR) spectroscopy is a crucial technique that we use not only to obtain structural information on our molecules at an atomic level[6–11] but, even more important, to elucidate in detail their metal ion binding.[2,9,10,12–18] Fig. 1 shows three examples of recently solved structures, belonging to the three families of biomolecules we are working with: the exon/intron binding site 1 (EBS1/IBS1; PDB ID 2K65)[19] of the yeast mitochondrial group II intron *Sc*.ai5γ, a silver modified duplex DNA (PDB ID 2KE8),[8] and the C-terminal domain of the seed-specific wheat MT Zn_6E_c-1, denoted as $Zn_4\beta_E$-E_c-1 (PDB ID 2KAK).[10]

The chemical institutes at the University of Zurich run a central NMR facility currently equipped with one 700, one 600, three 500, two 400, and one 300 MHz spectrometer. Three of the high-field machines (500, 600, and 700 MHz) are equipped with z-axis pulsed field gradient Cryoprobes™ (Bruker), and are used for classical structural biology experiments (2D and 3D experiments on ^{1}H, ^{13}C, ^{15}N nuclei, as well as ^{31}P). One 500 MHz spectrometer is dedicated to variable-temperature and multinuclear NMR studies. In particular, the latter machine is used for direct observation of NMR active metal nuclei, including for example ^{59}Co, $^{107/109}Ag$, $^{111/113}Cd$, and ^{199}Hg.

This review is divided into two parts. In the first part, we show which kind of information can be obtained by NMR in the field of metal ion–nucleic acid interactions. We focus on our progress in the field of metal ion interaction with large RNAs as well as discuss recent results on metal modified oligonucleotides. The second part of this review is dedicated to our recent results on the use of classical and metal NMR to characterize the metal clusters in plant MTs.

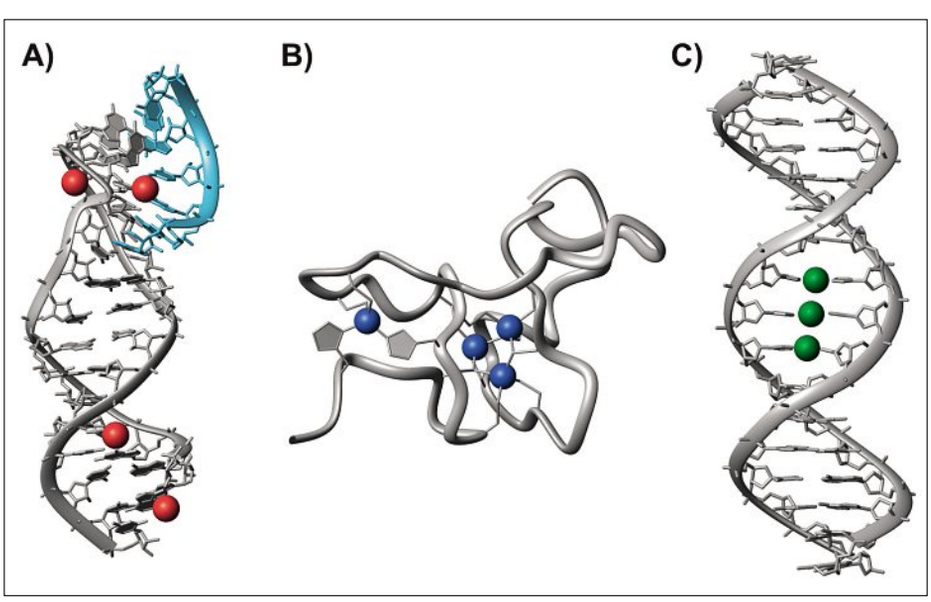

Fig. 1. NMR solution structures of (A) the intron-exon binding site of a group II intron ribozyme EBS1-IBS1 (PDB ID 2K65) including the positions of four Mg^{2+} ions (red spheres),[19] (B) the β_E-domain of the wheat metallothionein E_c-1, $Zn_4\beta_E$-E_c-1 (PDB ID 2KAK),[10] and (C) a modified DNA helix with three Ag^+ ions (green spheres) coordinated by pairs of imidazole nucleotides, respectively (PDB ID 2KE8).[8] This Figure has been prepared with MOLMOL[20] based on the given PDB files.

*Correspondence: Prof. Dr. E. Freisinger,
Prof. Dr. R. K. O. Sigel
University of Zurich
Institute of Inorganic Chemistry
Winterthurerstrasse 190
CH-8057 Zürich
Tel.: +41 44 635 4621/52
Fax: +41 44 635 6802
E-mail: freisinger@aci.uzh.ch, roland.sigel@aci.uzh.ch

2. Nucleic Acids

2.1 *Ribozymes*

The discovery of catalytically active RNAs (ribozymes) in the 1980s represents a milestone in RNA-related research.[21] New functions and roles of RNAs in living cells are constantly being discovered,[22] making RNA an attractive and intriguing object of study. Metal ions play a crucial role in RNA biochemistry: RNAs are polyanionic molecules and without metal ions neither a stable functional 3D structure would be attained nor activity would be accomplished.[16,23,24] Longer RNAs usually adopt complex three-dimensional structures. Majorly being present in a regular A-form double helix, such structures also contain a substantial amount of non-duplex secondary structural elements, *e.g.* bulges, loops, hairpins, and junctions.[25] Such non-canonical regions are often involved in tertiary contacts responsible for the global and local architecture of the RNA. Generally, these tertiary contacts are decisive for catalysis and often require stabilization by metal ions. Despite their crucial role, only little research is devoted to the understanding of the delicate interplay between RNA and metal ions.[16]

The study of group II intron ribozymes accounts for large parts of our research.[6,7,11,18,26–30] Group II introns with up to 2500 nucleotides in length are phylogenetically related to large parts of the eukaryotic genome and believed to be the direct ancestor of the eukaryotic spliceosome.[31] Group II introns are self-splicing ribozymes able to remove themselves, *i.e.* the intronic (non-coding) part, and to ligate the two flanking exons without the aid of proteins. Therefore, group II introns can reinsert themselves into RNA and DNA, behaving as mobile genetic elements. This characteristic makes them interesting candidates for medical applications. Group II introns are primarily found in organellar genes of plants, fungi, and lower eukaryotes, but also in bacteria. They largely lack sequence conservation, but are characterized by six domains radiating from a central wheel as well as conserved tertiary contacts.[31] Besides a background of monovalent metal ions used largely for neutralizing the highly negatively charged backbone, a certain amount of divalent metal ions is needed to attain the functional tertiary structure,[23,24,32] as well as to promote catalytic activity directly.[24]

Entire group II introns are too large to be investigated by NMR spectroscopy. However, they are modular in nature, and hence offer an optimal platform for the study of metal ion-RNA binding properties.[12,13,32] The single parts can be transcribed in large amounts,[33] studied independently, and their properties translated to the whole intron. For this reason we largely focus on single parts or domains of the yeast mitochondrial group II intron *Sc*.ai5γ being one the best investigated introns.[6,7,11,26] First, we solve the NMR structure of catalytically important parts of this intron, based on which we carry out a detailed evaluation of their metal ion interactions. New metal ion binding pockets and metal induced structural changes have been identified in our lab, as well as novel methods developed to quantify metal ion-RNA interactions.

2.1.1 *NMR as a Tool to Study Nucleic Acid Interaction with Metal Ions*

A strict evaluation of metal ion–RNA binding properties is essential for a better understanding of the catalytic activity of large ribozymes.[24] The most abundant and important metal ions associated with RNA are K^+, Na^+, Ca^{2+}, and Mg^{2+}, the latter being the natural RNA cofactor. While all four metal ions have NMR active isotopes, most of them show unfavorable properties, like low abundance and sensitivity as well as large quadrupolar moments, and only few reports have been published dealing with the NMR observation of these nuclei in biological systems.[34] As these metal ions are also not observable with most other spectroscopic techniques, they are considered spectroscopically silent, and hence often other metal ions are used to mimic their binding and function.[12] For example, innersphere binding properties of Mg^{2+}, *i.e.* the direct coordination of the metal ion to donor atoms of the nucleic acid, are studied using Cd^{2+} and Mn^{2+} as spectroscopic probes, while $[Co(NH_3)_6]^{3+}$ is employed to evaluate its outersphere binding properties, *i.e.* the hydrogen bonding of its first shell water molecules to the nucleic acid.

2.1.1.1 *Indirect Observation of Metal Ion Binding to RNA*

Due to the general problems to observe the metal ions directly as indicated above, monitoring chemical shift changes of the ligand is commonly applied to identify metal ion binding sites. RNA offers numerous potential coordinating atoms, such as phosphoryl oxygens, purine N7 and carbonyl oxygens.[16] To complicate matters, binding is usually intrinsically labile with metal ion–ligand exchange rates on the NMR time scale, *i.e.* milliseconds. Consequently, strong line broadening often hampers a detailed analysis. Nevertheless, both the chemical shift changes and the resonance broadening give direct evidence of metal ion binding to a specific site.

Nucleotide resonances close to a Mg^{2+} binding site are affected by Mg^{2+} addition: As a general rule, a contemporary shift and broadening suggests a direct coordination, while simple chemical shift change can be interpreted as a structural change of the wider binding pocket. Nevertheless, unequivocal interpretation of chemical shift changes is often difficult, as they usually are the result of several factors, *e.g.* the electron-withdrawing effect of the metal ion, increased solvent accessibility for imino protons, or changes in stacking interactions. Non-exchangeable protons are best suited for a detailed evaluation of metal-ion binding and consequently recording [^{1}H,^{1}H]-NOESY spectra at different Mg^{2+} concentrations is the method of choice (Fig. 2A).[4,6,7,14] Such experiments permit the chemical shift changes of the

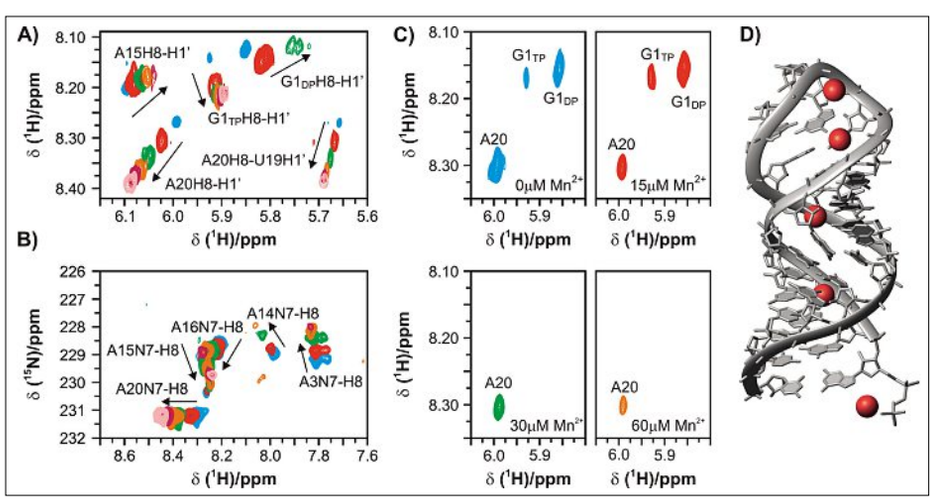

Fig. 2. Metal ion binding to a domain 6 construct of the yeast mitochondrial group II intron *Sc*.ai5γ (D6-27). Overlaid selected region of (A) [^{1}H,^{1}H]-NOESY[30] and (B) [^{1}H,^{15}N]-HSQC[18] spectra in the presence of increasing amounts of Mg^{2+} (0-10 mM (A) and 0-2.5 mM (B)). (C) Selected region of [^{1}H,^{1}H]-NOESY spectra in the presence of increasing amounts of Mn^{2+}. The assignment refers to the respective intranucleotide cross peaks H1'-H8. $G1_{DP}$ and $G1_{TP}$ indicate the diphosphate or triphosphate groups at the 5'-termini, respectively.[30] (D) NMR solution structure of D6-27 with five Mg^{2+} ions at their proposed sites shown as red spheres (PDB ID 2AHT)[6] prepared with MOLMOL.[20] Panels (A) and (C) are adapted from refs [14, 30]. Panel (B) is reprinted from ref. [18] with permission from Elsevier; copyright 2010.

non-exchangeable protons H8, H6, H5, H2, H1', and H2' to be followed unambiguously. This method can be even applied to larger RNA constructs if partially deuterated samples are used.[35] More details on individual coordinating atoms can also be gained: For example, shifts of the purine N7 resonance upon addition of increasing amounts of metal ions can be followed by recording ^2J-[^{1}H,^{15}N]-HSQC spectra on ^{15}N labeled RNA samples yielding a clear indication of metal ion coordination (Fig. 2B).[18]

However, [^{1}H,^{1}H]-NOESY as well as ^2J-[^{1}H,^{15}N]-HSQC experiments do not allow innersphere from outersphere coordination to be distinguished, binding modes that both are widely common.[36] As mentioned above, Cd^{2+} and Mn^{2+} are used to mimic innersphere binding. Cd^{2+} has a higher intrinsic affinity towards N atoms compared to Mg^{2+} and can lead to a ^{15}N chemical shift change of up to 20 ppm as observed, *e.g.* in a hammerhead ribozyme metal ion binding site model.[37] Mn^{2+} evidences direct binding by inducing paramagnetic line broadening of proton resonances in close proximity at already low concentration (<100 μM, Fig. 2C).[30]

Taken together, the various methods described above allow the ligand to be monitored in detail permitting sound conclusions with regard to location of the binding sites, innersphere vs outersphere binding, as well as related structural changes of the RNA.[11,18]

2.1.1.2 *Direct Observation of Metal Ion Binding to RNA using Spectroscopic Probes*

The kinetically inert complex $[Co(NH_3)_6]^{3+}$ is used to mimic the outersphere binding properties of $[Mg(H_2O)_6]^{2+}$.[12] Aside from the above described changes of the RNA chemical shifts, the observation of NOE cross peaks between its NH_3 protons and the protons of the RNA (Fig. 3) allows a direct localization of the metal ion binding site. Distance restraints deduced from these cross peaks can be included in the structure calculation.[11,38]

^{111}Cd and ^{113}Cd are two common isotopes both carrying the nuclear spin $^1/_2$. Consequently, [^{113}Cd]-NMR can be used to directly observe the metal ion: For example, large changes in chemical shift and broadening of the ^{113}Cd resonance was used to ascertain specific interactions to an RNA duplex.[39]

2.1.1.3 *Quantitative Analysis of the Data: Evaluation of the Intrinsic Affinity Constants*

In cases where the effects of metal ion binding and metal ion-induced structural rearrangements can be separated, the evaluation of chemical shift changes upon metal ion addition provides quantitative information of the thermodynamics of metal ion–RNA interaction. [^{1}H,^{1}H]-NOESY experiments are usually employed for this purpose: A series of experiments is recorded in the presence of different amounts of metal ions, and chemical shift changes of as many resonances as possible are plotted versus the respective metal ion concentration. These plots are then fit iteratively using a 1:1 binding model.[30] We have recently automated this iteration procedure using the Matlab® toolbox. This toolbox, named ISTAR®, allows intrinsic affinity constants to be calculated within seconds for each of the numerous binding sites usually found in a large RNA molecule starting solely from NMR chemical shift data.[40]

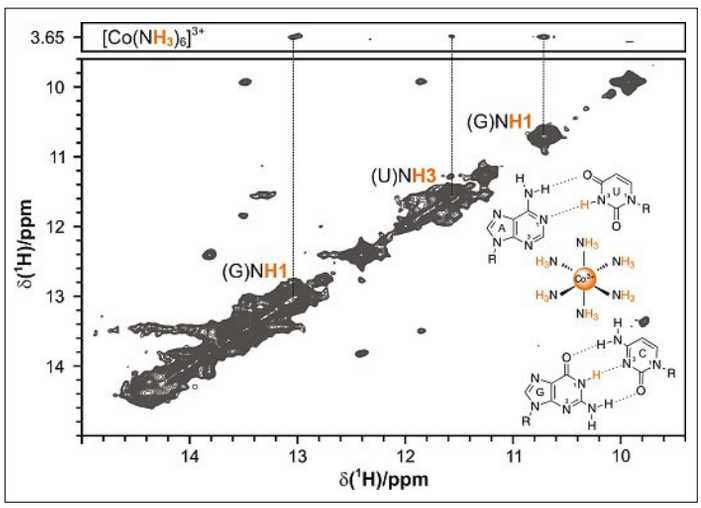

Fig. 3. Imino proton region of a [^{1}H,^{1}H]-NOESY spectrum of D1κζ in the presence of 0.4 mM $[Co(NH_3)_6]^{3+}$, showing the cross peaks between the NH_3 ligands and the imino protons (guanine NH1 and uracil NH3, see also inset).[11]

2.1.2 *A Case Study: Minimal Domain 6 (D6-27) of Group II Intron Ribozyme Sc.ai5γ*

Domain 6 of the group II intron plays a crucial role in the activity of the whole intron since it contains the branch point adenosine, whose 2'-OH group serves as the attacking nucleophile in the first step of splicing. In our group, the NMR solution structure of a truncated but still active domain 6 (D6-27)[6] was solved (Fig. 2D) and its metal ion binding properties were evaluated in detail.[18,30,40] [^{1}H,^{1}H]-NOESY experiments in the presence of increasing amounts of Mg^{2+} and Mn^{2+} were performed. Paramagnetic Mn^{2+} line broadening experiments suggested that the adenosine branch point is not directly involved in metal ion interaction. In fact, the intranucleotide A20H1'-H8 cross peak is almost unaffected by the addition of Mn^{2+} (Fig. 2C).[30] To confirm the absence of direct coordination to that site, ^2J-[^{1}H,^{15}N]-HSQC experiments were recorded with D6-27 containing ^{13}C,^{15}N labeled adenosines in the presence of increasing amounts of Mg^{2+}. Interestingly, neither chemical shift change nor line broadening of the N7 resonance of the branch-adenosine A20 was observed (Fig. 2B), supporting the hypothesis that no direct metal ion coordination to A20 takes place but rather a structural change within the binding pocket. This structural change is probably due to Mg^{2+} binding to the two GU wobble pairs neighboring A20 as revealed by corresponding ^2J-[^{1}H,^{15}N]-HSQC experiments of D6-27 containing ^{13}C,^{15}N labeled guanosines.[18]

Quantitative analysis of the chemical shift changes recorded by [^{1}H,^{1}H]-NOESY spectra (Fig. 2A) were performed[30] revealing the existence of four to five binding sites: The 5'-end of the hairpin, the GC tandem in the first helical region, the branch region, the tetraloop, and the helical region in immediate vicinity to the tetraloop (Fig. 2D). The $\log K_a$ values of the various binding sites all cluster around 2.1–2.2, corresponding to dissociation constants in the lower millimolar range. Higher $\log K_a$ values were found only at the 5'-end containing the terminal phosphate group(s).[30] The experimental data were recently re-evaluated with ISTAR®, with the aim of confirming the presence of one or two metal ion binding sites in the tetraloop region.[39] It was shown that the experimental data are better described using a model that considers only four metal ion binding sites, *i.e.* only one single metal ion is positioned in the tetraloop region and the neighboring helical region. This metal ion moves along a 14 Å long part of the RNA molecule. Reducing the total number of metal ion binding sites to fit the experimental data also results in higher calculated affinities of the remaining sites.

Taken together, a combination of the experiments described above allows a valid and powerful evaluation of metal ion binding to RNA and to obtain a detailed picture of large RNAs in combination with their crucial metal ion cofactors at the atomic level.

2.2 *Metal Ion-functionalized Nucleic Acids*

In the age of nanotechnology, nucleic acids became propitious candidates for structural frameworks of nanodevices due to their basic, iterative structural motives and their predictable self-assembly properties. The creation of complex and large 2D and 3D nanoarchitectures using nucleic acids is no longer a vision but a rather simple task by choosing the right sequences.[41] The site-specific modification of nucleic acids with metal ions using metal-mediated base pairs widens their application range even more and is a promising strategy to overcome the lack of sufficient conducting properties of natural nucleic acids.[42] In metal-mediated base pairs two nucleobases, which can be either natural or artificial, positioned on opposite strands are linked through coordinative bonds to a central metal ion in the core of the helix.[42,43]

Common metal ions applied to site-specifically functionalize nucleic acids are transition metal ions like Ni^{2+}, Cu^{2+}, Pd^{2+}, Mn^{2+}, Fe^{2+}, Hg^{2+}, and Ag^{+} that can in most cases be explored with either Mössbauer, EPR, or NMR spectroscopy. Especially the isotopes of mercury (^{199}Hg) and silver (^{107}Ag, ^{109}Ag) have appropriate NMR properties and can be observed either directly or indirectly through the coupling to other NMR active nuclei, *e.g.* ^{1}H, ^{13}C, ^{15}N, or ^{31}P.

The first preliminary NMR studies on such systems were accomplished on DNA duplexes containing mismatched thymidine residues. The results indicated that in the presence of Hg^{2+} ions linear T–Hg^{2+}–T base pairs are formed with the Hg^{2+} replacing the N3H protons of the thymine nucleobases.[44] Not until 40 years later, Tanaka *et al.* could finally prove this assumption using ^{15}N NMR spectroscopy.[45] Upon addition of Hg^{2+} ions the ^{15}N labeled N3 atoms of two opposite thymine residues reveal a strong downfield shift (about 30 ppm) as well as a splitting due to a ^{15}N-^{15}N *J*-coupling across Hg ($^{2}J_{NN}$) that can only be explained by the coordination of Hg^{2+} ions.

Our recent studies showed that also RNA sequences comprising 2, 3, 6, 10, and up to 20 consecutive uridine residues can incorporate Hg^{2+} ions into the helix forming U-Hg^{2+}-U base pairs without disturbing the A-helical structure.[17] To further investigate Hg^{2+} ion binding to uracils by NMR we focused on a palindromic 22 nt long RNA sequence with six successive uracil residues. In this case Hg^{2+} ion binding induces a structure conversion from hairpin to duplex causing not only a distinct change in chemical shifts but also of the size of the molecule. DOSY (diffusion-ordered spectroscopy) measurements of the RNA in the absence and presence of Hg^{2+} ions revealed a 30% increase of the hydrodynamic radius r_H upon addition of Hg^{2+} ions.[17] Next to [^{1}H,^{1}H]-NOESY and [^{1}H,^{1}H]-TOCSY spectra that were recorded to obtain structural information, also [^{199}Hg] and [^{15}N]-NMR experiments were conducted to directly prove the configuration of U-Hg^{2+}-U base pairs. All NMR spectra of the Hg^{2+}-modified RNA showed a general line broadening, but in particular for the resonances of the six consecutive uracils. As is quite commonly seen, also here [^{199}Hg]-NMR spectroscopy revealed no signals other than that of free Hg^{2+} ions, probably due to the following reasons: i) typically Hg^{2+} coordinates in a kinetically labile manner and thus exchanges fast and ii) CSA (chemical shift anisotropy) relaxation often causes a strong line broadening of the ^{199}Hg resonances. Therefore we focused on [^{15}N]-NMR spectroscopy using RNA with ^{13}C,^{15}N labeled uracils and recorded ^{3}J-[^{1}H,^{15}N]-HSQC spectra correlating the H5 protons of the uracil to the endocyclic nitrogen atoms N1 and N3 in the presence and absence of Hg^{2+} ions.[17] Except for the strong line broadening of the N3 resonances of the six consecutive uracil residues no further direct evidence like strong chemical shift changes or splitting of the N3 resonances as Tanaka *et al.*[45] found for their Hg^{2+} modified DNA could be observed.[17] This suggests that Hg^{2+} binding to RNA is markedly weaker compared to DNA, which is most likely caused by the distinct different helical structures of RNA and DNA.

A further example of such metal-modified nucleic acids investigated in our group using multitudinous heteronuclear NMR experiments, is a 17 nt long DNA containing three imidazole (Im) moieties as nucleobase surrogates.[8] At neutral pH and in the absence of Ag^{+} ions the self-complementary DNA forms a stable hairpin comprising the artificial bases in an unstructured loop. Upon binding of Ag^{+} ions the DNA undergoes a structure conversion from hairpin to duplex positioning the three silver mediated imidazole base pairs in the middle (Fig. 1C). 2D [^{1}H]-NMR spectra reveal that the addition of Ag^{+} ions leads to major chemical shift changes and narrowing of the resonances belonging to the imidazole moieties. This indicates a rigid structure around the imidazole nucleotides as is expected for the formation of Im-Ag^{+}-Im base pairs. Again, this conversion from hairpin to duplex is accompanied by a distinct increase in size. The determination of the hydrodynamic radii by DOSY yielded r_H = 1.5 nm for the metal-free DNA and r_H = 1.9 nm for the DNA in the presence of Ag^{+} ions. These values perfectly match the theoretical calculated radii. As no ^{109}Ag signals were observed in additionally measured [^{1}H,^{109}Ag]-HMQC spectra,[46] we inserted ^{15}N labeled Im bases into our DNA and performed long-range [^{1}H,^{15}N]-HSQC experiments to obtain a final proof for the presence of Im-Ag^{+}-Im base pairs within the helix.[8] In the metal-free DNA the correlation of N1 and N3 to the three aromatic protons H2, H4, and H5 (Fig. 4A) yielded only a few not very well-resolved cross-peaks clustering around 188 ppm (N1) and around 221 ppm (N3). Upon addition of Ag^{+} ions all expected ^{1}H-^{15}N crosspeaks became visible and the N3 resonances experienced an upfield shift of $\Delta\delta \approx -15$ ppm while the N1 resonances shifted only slightly by about –3 ppm. This strong upfield shift of the N3 resonances suggests direct coordination of Ag^{+} ions. Most importantly, the N3 resonances displayed a splitting of 86 Hz, which can be attributed to a direct coupling between the nitrogen and the silver atoms, *i.e.* a ^{1}J(^{15}N,$^{107/109}$Ag) coupling (Fig. 4B). This large coupling is not only a direct evidence for the three metal-mediated base pairs but verifies that the metal exchange reaction is very slow. Consequently, the Ag^{+} ions must be tightly bound to the artificial nucleosides and be well embedded within the double helical structure.[8] In general, ^{1}J(^{15}N,$^{107/109}$Ag) coupling constants are observed rarely in solution because Ag^{+} ions usually bind to nitrogen donors in a highly labile fashion and no coupling can be observed. In theory it should be possible to distinguish the ^{1}J(^{15}N,^{107}Ag) and ^{1}J(^{15}N,^{109}Ag) couplings in [^{15}N]-INEPT (insensitive nuclei enhanced by polarization transfer) experiments.[47] Although this did not work in the present

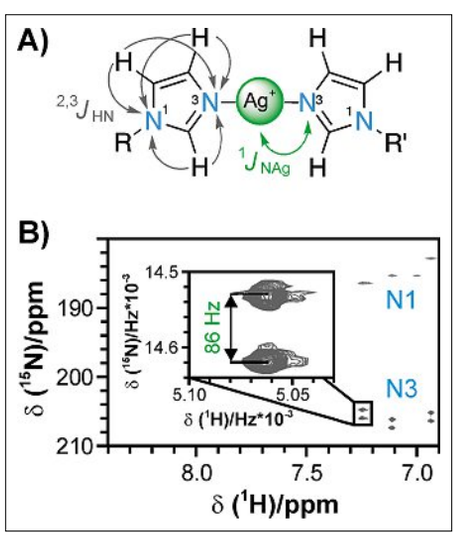

Fig. 4. Direct evidence for the formation of Im-Ag^{+}-Im base pairs. (A) Chemical structure showing the connectivities within the metal-mediated base pair and the various couplings observed. The ^{1}J(^{15}N,$^{107/109}$Ag) coupling is shown in green. (B) Section of the [^{1}H,^{15}N]-HSQC with the magnification of the Im8 N3-H2 and N3-H5 cross-peaks illustrating the ^{1}J(^{15}N,$^{107/109}$Ag) coupling of 86 Hz. This figure is adapted from ref. [8].

case because of strong overlap of the N3 signals, the larger line width of N3 (17 Hz) compared to N1 (7 Hz) clearly indicates the presence of both couplings. Taking together, a detailed picture of the metallated duplex with the Ag^+ ions being incorporated along the helical axis without inducing major conformational distortions of the B-helical type structure was obtained.[8]

Even though a rapid development in the field of metal-functionalized nucleic acids is taking place detailed structural information is still rare. However, our recent results clearly reveal that even if it is not possible to directly observe the coordinating metal ions by NMR, indirect methods can still give valuable information that is important for a better understanding of these systems.[4,12,14,48]

2.3 *Nucleic Acid Interactions with Metal Complexes*

Transition metal complexes can interact with nucleic acids, and these interactions are very different from those of metal ions only. There are two main interaction modes between metal complexes and nucleic acids: covalent and non-covalent binding. The covalent interaction is led by the metal center, which binds to oxygen or nitrogen atoms of the nucleobases, or to phosphate oxygens. Contrarily, the nature of non-covalent binding is defined by the primary ligand of the metal ion and can be of different kinds: i) electrostatic interaction with the phosphate backbone, ii) hydrophobic groove binding, iii) hydrogen bonding between the ligand and the nucleic acid, iv) intercalation, and v) insertion.[49]

NMR spectroscopy has been extensively used over the past years to evaluate the binding mode of metal complexes to nucleic acids. For example, [^{1}H,^{15}N]-HSQC experiments were used to obtain insights into the mechanism of action of platinum drugs, including kinetics and selectivity of DNA platination reactions.[50] Also [^{195}Pt]-NMR can provide important information on platination reactions, since the ^{195}Pt chemical shift range spans thousands of ppm and is particularly sensitive to changes in the coordination sphere.[50] In addition, NMR spectroscopy was used to solve the structure of platinated double stranded DNA as well as to evaluate the intercalative mode of interaction between metal complexes and DNA.[50,51]

Metal complexes have numerous possible applications, ranging from diagnosis to therapeutics.[52] Given the increasing importance of RNA as possible alternative molecular target for several drugs,[53] we have recently started as part of an Ambizione Fellowship (to DD) and within the COST Action CM1105 to evaluate the interaction between metal-based drugs and RNA molecules using different techniques, including multinuclear NMR spectroscopy.

3. Plant Metallothioneins

MTs are a class of small cysteine-rich proteins that occur in the most diverse living organisms, *e.g.* vertebrates, bacteria, fungi, and plants. Induced by the high cysteine content, they preferentially coordinate soft metal ions with the electron configuration d^{10} in form of metal–thiolate clusters. Owing to the high affinity of MTs towards Zn^{2+}, Cu^+, Cd^{2+}, and Hg^{2+} ions they are thought to be involved in metal ion homeostasis and detoxification. Their high cysteine content led to the proposal that they might have an additional role in the protection against reactive oxygen species. Due to a lack of secondary structural elements the overall structure of MTs is mainly governed by the metal–thiolate cluster formation. As often only the parts of the amino acid sequence that are directly involved in metal binding reveal well-defined structures, it turns out that structure determination of MTs, both by X-ray crystallography and NMR, is a rather challenging task. This is especially true for certain plant MTs as they contain larger Cys-free regions that are not involved in metal ion coordination and hence more flexible. Until recently, only two major cluster arrangements for divalent metal ions were structurally characterized: the $M_4^{II}Cys_{11}$ and the $M_3^{II}Cys_9$ cluster, which can be both found, *e.g.* in vertebrate MTs (Fig. 5A,B). In certain MTs also histidine residues participate in metal cluster formation. Beside some common characteristics shared by all members of the MT superfamily, plant MTs feature a number of unique properties such as higher sequence diversity, occurrence of aromatic amino acids including histidine, and long Cys-free amino acid stretches as mentioned above.[1–3] Not surprisingly, this variety is also reflected on the structural level as the first structure elucidation of a plant MT, *i.e. Triticum aestivum* (common bread wheat) Zn_6E_c-1, revealed two metal ion arrangements that were both unprecedented for MTs at that time.[9,10] The C-terminal β_E-domain exposes a mononuclear binding site, $M^{II}Cys_2His_2$, intertwined with the residues forming a $M_3^{II}Cys_9$ cluster (Fig. 1B), while the smaller N-terminal γ-domain forms a $M_2^{II}Cys_6$ cluster (Fig. 5C).

Due to the importance of the metal ion coordination for the overall structure of the MT, it is crucial to precisely elucidate the metal–thiolate cluster structure formed. Apart from X-ray crystallography, heteronuclear NMR and in particular metal NMR is the only method that can give such detailed insights.

The essential metal ions coordinated by MTs are Zn^{2+} and Cu^+. However, these metal ions do not have any applicable NMR properties. Nevertheless, there are a number of nuclei with similar coordination properties that are suitable for NMR, *e.g.* $^{107/109}$Ag, $^{111/113}$Cd, and ^{199}Hg. Cd^{2+} is frequently used to mimic Zn^{2+} as it prefers the same tetrahedral coordination mode. It offers two isotopes, 111 and 113, that are suitable for NMR measurements both having a nuclear spin of ½. The $^{111/113}$Cd chemical shift alone already gives valuable information as it is sensitive to the nature, number, and geometric arrangement of the coordinating ligands and covers a chemical shift range of about 900 ppm.[55] For example the 1D [^{113}Cd]-NMR spectrum of the Cd_6E_c-1 form displays only signals between 650–700 ppm indicating that all observable resonances are in the usual range for tetrahedral tetrathiolate coordination (600–700 ppm) (Fig. 6A).[15] Although E_c-1 has the ability to bind six $^{113}Cd^{2+}$ ions, only five resonances were visible most likely due to a smaller affinity of $^{113}Cd^{2+}$ towards the mononuclear N_2S_2 site. With [^{113}Cd,^{113}Cd]-COSY experiments direct coupling of metal ions can be observed and hence allows the identification of metal ions that belong to the same cluster.[55] In

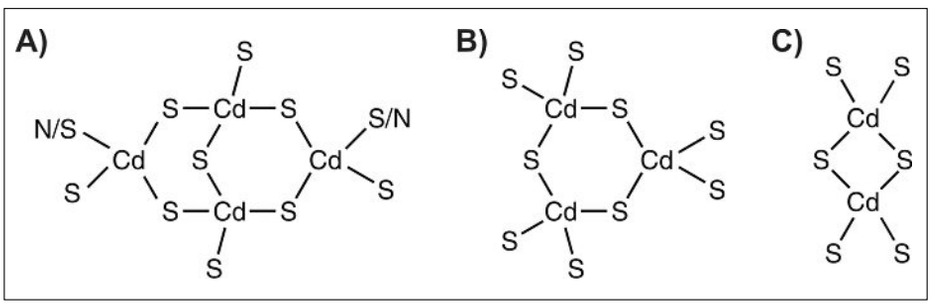

Fig. 5. Metal–thiolate cluster structures found in MTs in the presence of divalent metal ions. Depicted are the two major cluster arrangements $M_4^{II}Cys_{11}$ of the α-domain (A) and $M_3^{II}Cys_9$ of the β-domain (B), which can be both found *e.g.* in vertebrate MTs as well as the $M_2^{II}Cys_6$ cluster (C) that was recently discovered in the γ-domain of the plant MT E_c-1.[2,9] In certain MTs also His ligands can participate in metal ion coordination, *e.g.* in the $M^{II}_4Cys_9His_2$ cluster found in bacterial MTs (A).[54]

the case of Cd_6E_c-1 cross peaks between the two most intense signals were found (659–661 ppm) originating from the two $^{113}Cd^{2+}$ ions of the γ-domain (Fig. 6B). It was not possible to observe cross peaks for the $M_3^{II}Cys_9$ cluster of the β_E-domain due to the much larger line width of these ^{113}Cd resonances compared to the ones of the γ-domain.[15] To established metal–thiolate connectivities [^{1}H,^{113}Cd]-HSQC experiments are required that correlate the ^{113}Cd resonance to the CH^β protons of the cysteine ligands. This vicinal $^1H^\beta$,^{113}Cd-cysteine coupling follows in many cases a Karplus-type dependence and therefore can be used to determine the H^β-C^β-S-Cd dihedral angles important for structure calculation. In Fig. 6C the [^{1}H,^{113}Cd]-HSQC spectrum of the isolated γ-domain of E_c-1 is depicted that in combination with structure determination studies identifies Cys-9 as one bridging cysteine and indicates the presence of a highly dynamic metal cluster, switching between Cys-3 and Cys-21 as second bridging thiolate ligand.[9] The [^{1}H,^{113}Cd]-HSQC-TOCSY, a combination of a hetero- and homonuclear experiment, links the $^{113}Cd^{2+}$ ion not only to the CH^β protons but also to the CH^α and NH protons of the cysteine residues. Such enhanced signal dispersion largely simplifies the unambiguous assignment of Cys-Cd connectivity.[56] ^{113}Cd is by far the most applied metal nuclei for NMR studies in biological systems, however also ^{199}Hg has excellent NMR properties. In particular, the large chemical shift range of about 1300 ppm enhances the sensitivity for the primary coordination sphere even further compared to the ^{113}Cd nucleus. As Hg^{2+} often readily exchanges native Zn^{2+} and Cu^+ ions [^{1}H,^{199}Hg]-HSQC experiments were used to probe metal ion coordination in native and *de novo* designed metalloproteins.[57,58] In addition, also monovalent Cu^+ ions can be mimicked using [^{109}Ag]-NMR. Nevertheless, up to date only in the case of the silver-substituted yeast metallothionein CUPI [^{1}H,^{109}Ag]-HMQC experiments were successfully applied to identify the individual ^{109}Ag resonances and their associated cysteine ligands.[46] It has to be noted however, that certain differences in the coordination modes of Cu^+ and Ag^+ were observed, and hence the use of Ag^+ for isostructural replacement of Cu^+ ions has to be evaluated with caution.

Last, but not least, also indirect methods can be used to probe the metal cluster of certain MTs. For example to establish His coordination of metal ions, long-range [^{1}H,^{15}N]-HSQC spectra can be employed as the ^{15}N chemical shift is sensitive towards protonation, hydrogen bonding, and metal coordination. The [^{1}H,^{15}N]-HSQC spectrum of $Zn_4\beta_E$-E_c-1 (Fig. 7) indicates metal ion binding to the His residues and was used to determine the tautomeric forms of the two histidines.[10]

Up to now, NMR spectroscopy is one of the most powerful methods to obtain detailed insights in the structure and function of the fascinating class of metallothioneins using homonuclear but also heteronuclear NMR techniques. Historically, MTs were actually among the first proteins studied by NMR and used to develop and establish the technique for the study of proteins.[59,60] Nevertheless, there is still a huge number of MTs with most diverse sequences awaiting analysis and structural elucidation, and it is most likely that NMR spectroscopy will remain to be one of the major methods of choice.

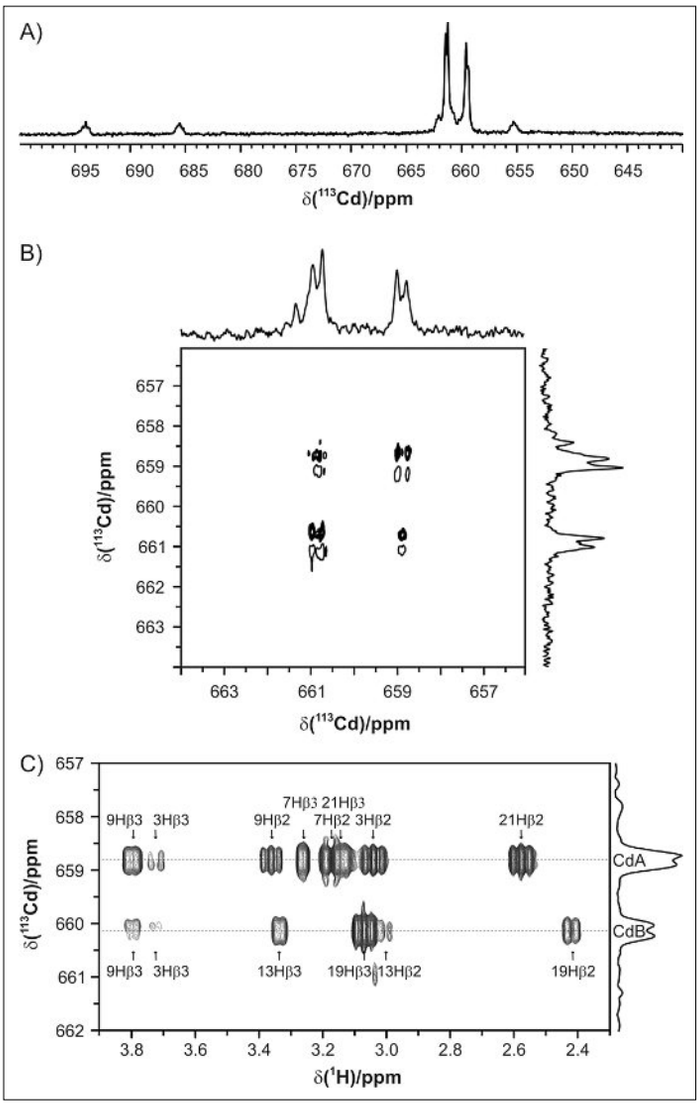

Fig. 6. Cd^{2+} binding to a metallothionein. (A) 1D [^{113}Cd]-NMR and (B) [^{113}Cd,^{113}Cd]-COSY spectra of $^{113}Cd_6E_c$-1. The latter shows the cross peaks (659-661 ppm) between the two most intense peaks of the spectrum shown in (A), which originate most likely from the two $^{113}Cd^{2+}$ ions coordinated in the γ-domain of E_c-1. (C) [^{1}H,^{113}Cd]-HSQC spectrum of the isolated γ-domain of E_c-1 showing the assignments obtained through CH^β-^{113}Cd connectivities. Panels (A) and (B) are reprinted from ref. [15] with permission from Elsevier; copyright 2009.

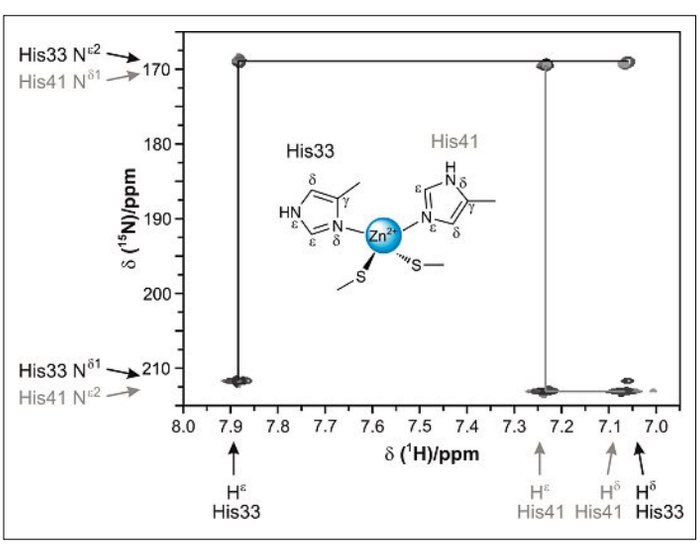

Fig. 7. Long-range [^{1}H,^{15}N]-HSQC of $Zn_4\beta_E$-E_c-1 to determine the tautomeric forms of the two His ligands. The peak pattern reveals that His33 is in its $N^{\varepsilon 2}$-H tautomeric form, while His41 is present as $N^{\delta 1}$-H tautomer suggesting that $N^{\delta 1}$ of His33 and $N^{\varepsilon 2}$ of His41, respectively, are coordinating the Zn^{2+} ion. Adapted from ref. [10] with permission from Elsevier; copyright 2009.

4. Conclusions

Metal ions play crucial roles in living cells. NMR spectroscopy provides numerous highly useful applications and tools to elucidate the roles of metal ions in proteins and nucleic acids. This bioinorganic chemical aspect of Life is the research focus of our laboratories. Ribozymes, nucleic acids in general, as well as metallothioneins provide a fascinating platform to investigate the fundamental interactions between metal ions and these large biomolecules. Based thereon, folding, structure, and function governed by metal ions is investigated and provides us with the knowledge to understand fundamental processes of Life as well as to transfer this knowledge to future applications in Medicine and Nanotechnology.

Acknowledgement

Eva Freisinger and Roland Sigel thank all their past and present group members for their hard work, enthusiasm, and great atmosphere in the lab, as well as many colleagues and friends from across the world for very fruitful collaborations. Financial support by the Swiss National Science Foundation (*SNSF-Professorship* to EF, Marie Heim-Vögtlin Fellowship to SJ, Ambizione Fellowship to DD, as well as individual project support to RKOS), the European Research Council (ERC Starting Grant to RKOS), the State Secretariat for Education and Research (COST), and the University of Zürich is gratefully acknowledged.

Received: August 1, 2012

[1] E. Freisinger, *Dalton Trans*. **2008**, 6663.
[2] E. Freisinger, *Chimia* **2010**, *64*, 217.
[3] E. Freisinger, *J. Biol. Inorg. Chem.* **2011**, *16*, 1035.
[4] M. C. Erat, R. K. O. Sigel, *Met. Ions Life Sci.* **2011**, *9*, 37.
[5] R. K. O. Sigel, S. Gallo, *Chimia* **2010**, *64*, 126.
[6] M. C. Erat, O. Zerbe, T. Fox, R. K. O. Sigel, *ChemBioChem* **2007**, *8*, 306.
[7] R. K. O. Sigel, D. G. Sashital, D. L. Abramovitz, A. G. PalmerIII, S. E. Butcher, A. M. Pyle, *Nat. Struct. Mol. Biol.* **2004**, *11*, 187.
[8] S. Johannsen, N. Megger, D. Böhme, R. K. O. Sigel, J. Müller, *Nat. Chem*. **2010**, *2*, 229.
[9] J. Loebus, E. A. Peroza, N. Blüthgen, T. Fox, W. Meyer-Klaucke, O. Zerbe, E. Freisinger, *J. Biol. Inorg. Chem.* **2011**, *16*, 683.
[10] E. A. Peroza, R. Schmucki, P. Güntert, E. Freisinger, O. Zerbe, *J. Mol. Biol.* **2009**, *387*, 207.
[11] D. Donghi, M. Pechlaner, C. Finazzo, B. Knobloch, R. K. O. Sigel, **2012**, in revision.
[12] S. Johannsen, M. M. T. Korth, J. Schnabl, R. K. O. Sigel, *Chimia* **2009**, *63*, 146.
[13] M. C. Erat, R. K. O. Sigel, *Chimia* **2005**, *59*, 817.
[14] D. Donghi, R. K. O. Sigel, *Methods Mol. Biol.* **2012**, *848*, 253.
[15] E. A. Peroza, A. Al Kaabi, W. Meyer-Klaucke, G. Wellenreuther, E. Freisinger, *J. Inorg. Biochem*. **2009**, *103*, 342.
[16] E. Freisinger, R. K. O. Sigel, *Coord. Chem. Rev*. **2007**, *251*, 1834.
[17] S. Johannsen, S. Paulus, N. Düpre, J. Müller, R. K. O. Sigel, *J. Inorg. Biochem*. **2008**, 1141.
[18] M. C. Erat, H. Kovacs, R. K. O. Sigel, *J. Inorg. Biochem.* **2010**, *104*, 611.
[19] D. Kruschel, R. K. O. Sigel, 'NMR solution structure of the exon/intron binding site 1 (EBS1/IBS1) of the group II intron Sc.ai5(gamma)', doi: 10.2210/pdb2k65/pdb.
[20] R. Koradi, M. Billeter, K. Wüthrich, *J. Mol. Graph*. **1996**, *14*, 29.
[21] K. Kruger, P. J. Grabowski, A. J. Zaug, J. Sands, D. E. Gottschling, T. R. Cech, *Cell* **1982**, *31*, 147.
[22] R. F. Gesteland, T. R. Cech, J. F. Atkins, 'The RNA World', Cold Spring Harbor Press, **2006**.
[23] D. Donghi, J. Schnabl, *Met. Ions Life Sci*. **2011**, *9*, 197.
[24] R. K. O. Sigel, A. M. Pyle, *Chem. Rev.* **2007**, *107*, 97.
[25] S. E. Butcher, A. M. Pyle, *Acc. Chem. Res.* **2011**, *44*, 1302.
[26] R. K. O. Sigel, A. Vaidya, A. M. Pyle, *Nat. Struct. Biol*. **2000**, *7*, 1111.
[27] M. Steiner, K. S. Karunatilaka, R. K. O. Sigel, D. Rueda, *Proc. Natl. Acad. Sci. USA* **2008**, *105*, 13853.
[28] M. Steiner, D. Rueda, R. K. O. Sigel, *Angew. Chem., Int. Ed.* **2009**, *48*, 9739.
[29] M. C. Erat, R. K. O. Sigel, *J. Biol. Inorg. Chem*. **2008**, *13*, 1025.
[30] M. C. Erat, R. K. O. Sigel, *Inorg. Chem.* **2007**, *46*, 11224.
[31] A. M. Pyle, *Crit. Rev. Biochem. Mol. Biol.* **2010**, *45*, 215.
[32] R. K. O. Sigel, *Eur. J. Inorg. Chem.* **2005**, 2281.
[33] S. Gallo, M. Furler, R. K. O. Sigel, *Chimia* **2005**, *59*, 812.
[34] L. Ronconi, P. J. Sadler, *Coord. Chem. Rev*. **2008**, *252*, 2239.
[35] K. Lu, Y. Miyazaki, M. F. Summers, *J. Biomol. NMR* **2010**, *46*, 113.
[36] J. Schnabl, P. Suter, R. K. O. Sigel, *Nucleic Acids Res*. **2011**, *40*, 434.
[37] Y. Tanaka, K. Taira, *Chem. Commun*. **2005**, 2069.
[38] S. Rudisser, I. Tinoco, *J. Mol. Biol.* **2000**, *295*, 1211.
[39] M. Vogtherr, S. Limmer, *FEBS Lett*. **1998**, *433*, 301.
[40] M. C. Erat, J. Coles, C. Finazzo, B. Knobloch, R. K. O. Sigel, *Coord. Chem. Rev.* **2012**, *256*, 279.
[41] E. Stulz, G. Clever, M. Shionoya, C. Mao, *Chem. Soc. Rev*. **2011**, *40*, 5633.
[42] G. H. Clever, M. Shionoya, *Met. Ions Life Sci.* **2012**, *10*, 269.
[43] D. A. Megger, N. Megger, J. Müller, *Met. Ions Life Sci*. **2012**, *10*, 295.
[44] S. Katz, *Biochim. Biophys. Acta* **1963**, *68*, 240.
[45] Y. Tanaka, S. Oda, H. Yamaguchi, Y. Kondo, C. Kojima, A. Ono, *J. Am. Chem. Soc.* **2007**, *129*, 244.
[46] S. S. Narula, R. K. Mehra, D. R. Winge, I. M. Armitage, *J. Am. Chem. Soc*. **1991**, *113*, 9354.
[47] G. A. Morris, R. Freeman, *J. Am. Chem. Soc*. **1979**, *101*, 760.
[48] M. Pechlaner, R. K. O. Sigel, *Met. Ions. Life Sci.* **2012**, *10*, 1.
[49] M. J. Hannon, *Chem. Soc. Rev*. **2007**, *36*, 280.
[50] S. J. Berners-Price, L. Ronconi, P. J. Sadler, *Prog. Nucl. Magn. Reson. Spectrosc.* **2006**, *49*, 65.
[51] B. M. Zeglis, V. C. Pierre, J. K. Barton, *Chem. Commun.* **2007**, 4565.
[52] Z. J. Guo, P. J. Sadler, *Angew. Chem., Int. Ed*. **1999**, *38*, 1513.
[53] E. G. Chapman, A. A. Hostetter, M. F. Osborn, A. L. Miller, V. J. DeRose, *Met. Ions Life Sci*. **2011**, *9*, 347.
[54] C. A. Blindauer, M. D. Harrison, J. A. Parkinson, A. K. Robinson, J. S. Cavet, N. J. Robinson, P. J. Sadler, *Proc. Natl. Acad. Sci. USA* **2001**, *98*, 9593.
[55] G. L. Öz, D. L. Pountney, I. M. Armitage, *Biochem. Cell Biol*. **1998**, *76*, 223.
[56] A. Muñoz, F. H. Försterling, C. F. I. Shaw, D. H. Petering, *J. Biol. Inorg. Chem.* **2002**, *7*, 713.
[57] L. M. Utschig, J. W. Bryson, T. V. O'Halloran, *Science* **1995**, *268*, 380.
[58] O. Iranzo, P. W. Thulstrup, S.-b. Ryu, L. Hemmingsen, V. L. Pecoraro, *Chem. Eur. J.* **2007**, *13*, 9178.
[59] M. H. Frey, G. Wagner, M. Vasák, O. W. Sørensen, D. Neuhaus, E. Woergoetter, J. H. R. Kägi, R. R. Ernst, K. Wüthrich, *J. Am. Chem. Soc.* **1985**, *107*, 6847.
[60] G. Wagner, D. Neuhaus, E. Worgotter, M. Vasák, J. H. R. Kägi, K. Wüthrich, *Eur. J. Biochem*. **1986**, *157*, 275.